Supporting Information of-

rC14: Engineering a New Dual-Function Carbon Allotrope for Sustainable Energy Technologies under Conventional and Micro-strain Conditions

Yaru Wei[a,b,c,+], Baocheng Yang[b,+], Shouren Zhang[b], Houyang Chen[a,c]*

[a] *Chongqing Institute of Green and Intelligent Technology, Chinese Academy of Sciences, Chongqing 400714, P. R. China.*

[b] *Henan Provincial Key Laboratory of Nanocomposites and Applications, Institute of Nanostructured Functional Materials, Huanghe Science and Technology College*

[c] *Chongqing School, University of Chinese Academy of Sciences, Chongqing 400714, P. R. China.*

*Email: chenhouyang@cigit.ac.cn (H. Chen)

+ The authors contributed equally to this work.

Section S1. Equilibrium structural parameters of *RC14* and Validation of the theoretical calculations

The structural of the rC14 sheet are calculated using density functional theory as implemented in the Vienna Ab initio Simulation Package (VASP).[1] We note that there exists five different C-C bond lengths in rC14, which are C1-C2=1.39 Å, C2-C3=1.38 Å, C3-C4=1.44 Å, C3-C5=1.44 Å, C4-C4=1.39 Å, respectively. These bond lengths is similar with graphene (1.420 Å),[2] showing sp^2 hybridizing bonds character. There are also five different C-C bond angles in rC14, 111°for $\Theta_{C2\text{-}C3\text{-}C4}$, 124°for $\Theta_{C3\text{-}C3\text{-}C4}$, 111°for $\Theta_{C3\text{-}C4\text{-}C3}$, 109°for $\Theta_{C3\text{-}C5\text{-}C5}$, 105°for $\Theta_{C5\text{-}C3\text{-}C4}$, which are close to the 109.5° and 120° in graphene[2] and diamond[3] The detailed structural information of rC14 and structural parameters of other 2D carbon allotropes calculated are summarized in Table S1. The calculated results are in good agreement with previous theoretical and experimental, which confirms the reliability and accuracy of our calculation.

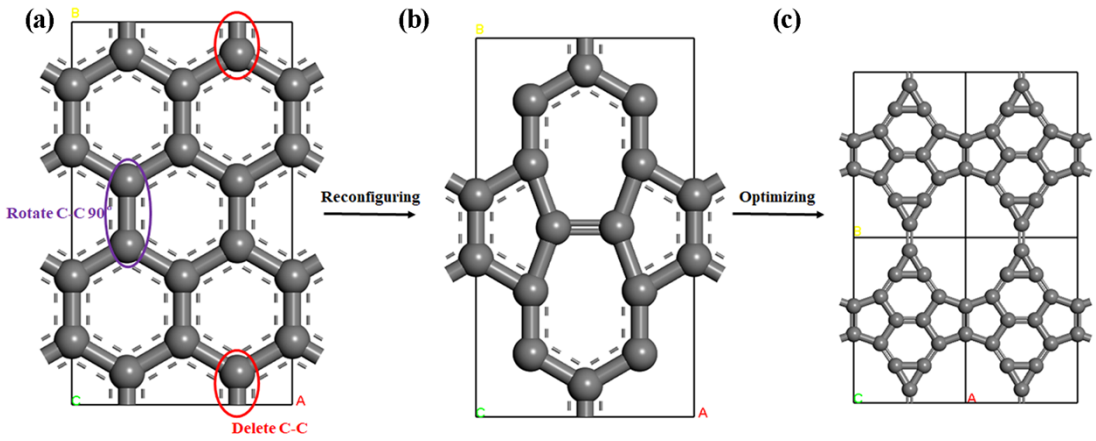

Figure S1. The pathway of defect-induced phase transition. (a) The optimized structure of pristine graphene; (b) the unoptimized structure of reconfiguring graphene; (c) the optimized structure (i.e. rC14).

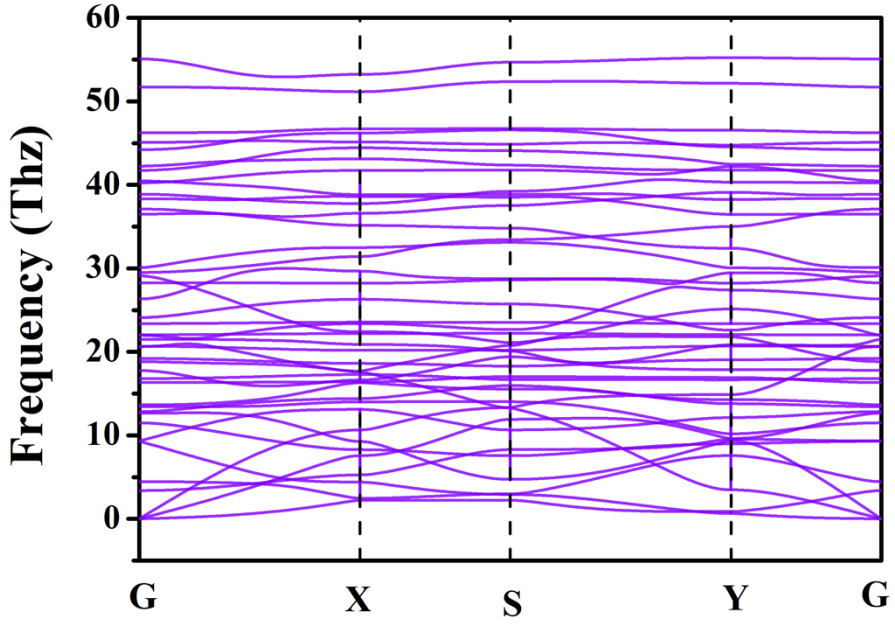

Figure S2. The phonon spectrum of rC14.

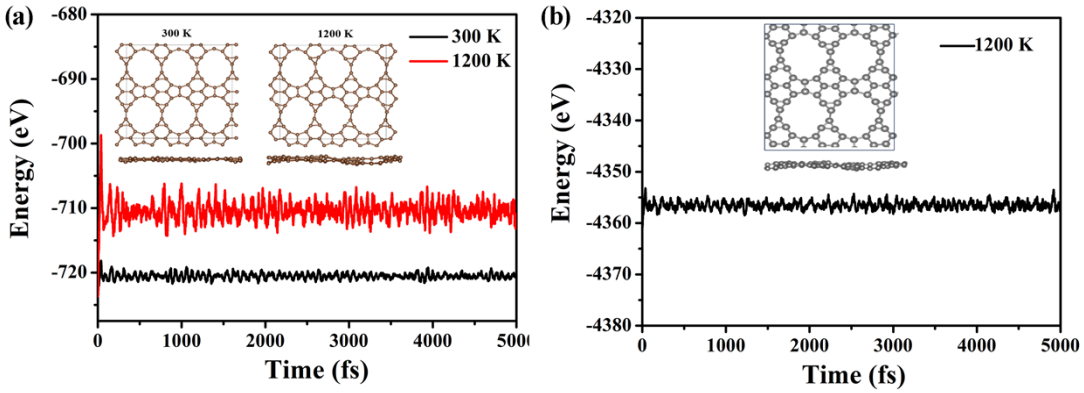

Figure S3. (a) Fluctuations of the total potential energy of rC14 at 300 and 1200 K performed by VASP. (b) Fluctuations of the total potential energy of rC14 at 1200 K performed by DS-PAW. Insets are snapshots of the structure at 5 ps.

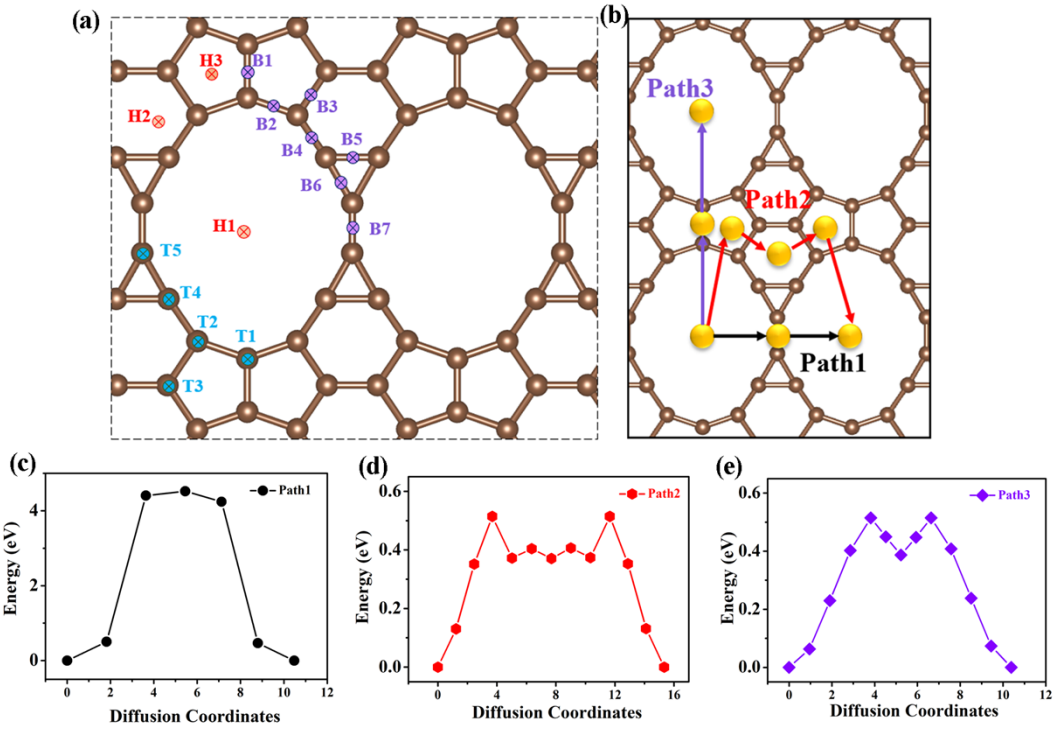

Figure S4. (a) Na adsorption sites on rC14. Red, purple and blue dots represent the hollow, bridge and top sites, respectively. (b) The three possible migration paths, and (c-e) the migration barrier of Na atom diffusion on rC14.

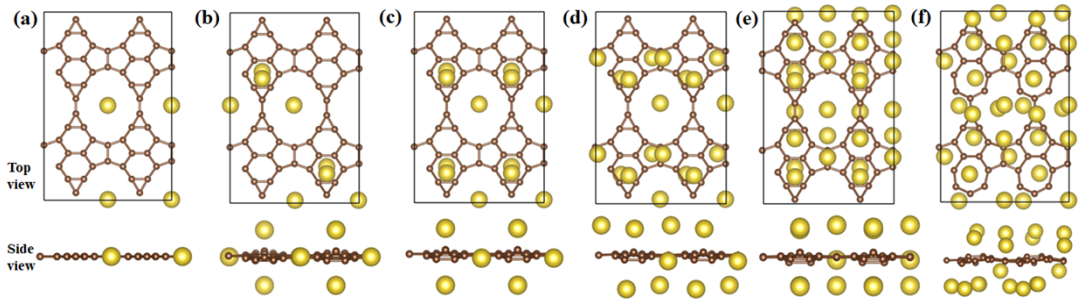

Figure S5. Top (upper) and side (below) views of the most stable configurations for the different concentration Na atoms adsorption on a rC14 monolayer, (a) Na4C_{56} (b)Na_8C_{56} (c)$Na_{12}C_{56}$ (d)$Na_{20}C_{56}$ (e)$Na_{28}C_{56}$(f) $Na_{32}C_{56}$.

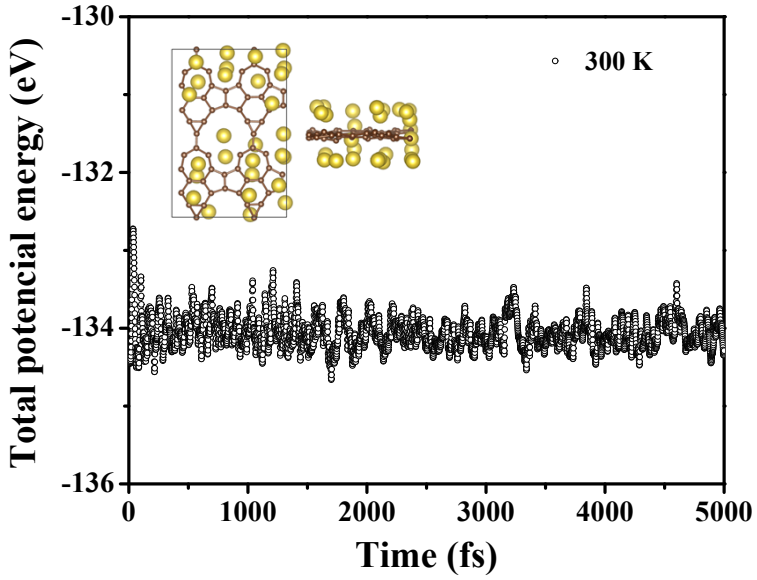

Figure S6. The total potential energies for twenty-eight Na atoms adsorption on a rC14 monolayer ($Na_{28}C_{56}$) at 300 K. Insets are the corresponding snapshots at the end of simulations.

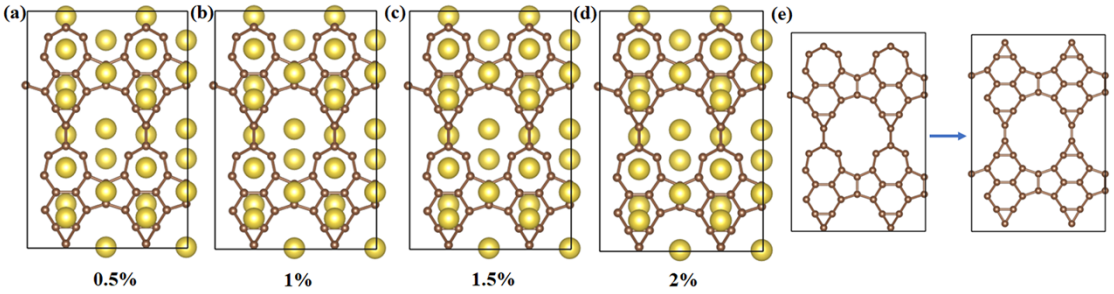

Figure S7. The structures of $Na_{28}C_{56}$ under the uniaxial compress strain along the under uniaxial and biaxial directions loading at 0.5%(a), 1%(b), 1.5%(c) and 2%(d). (e) the rC14monolayer of strain-induced phase transition.

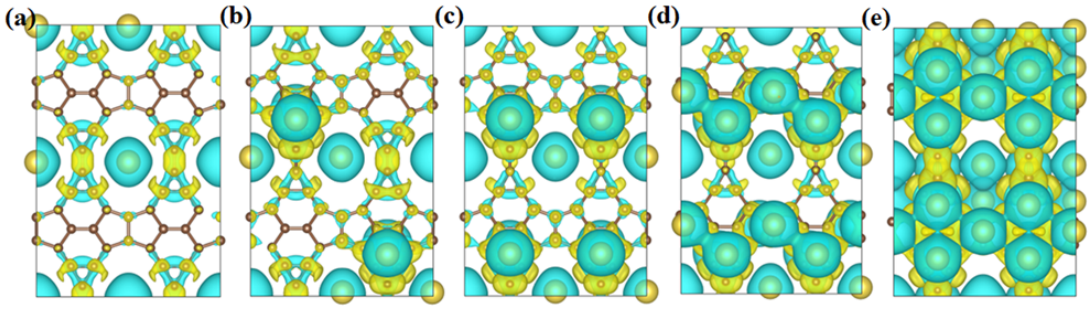

Figure S8. (a) Top views of charge density difference between the different concentration Na atom adsorbed on a *RC14* monolayer, (a) Na_4C_{56} (b)Na_8C_{56} (c)$Na_{12}C_{56}$ (d)$Na_{20}C_{56}$ (e)$Na_{28}C_{56}$. rC14with an isosurface value of 0.003 e/Bohr3. The yellow and blue colors represent charge gain and loss, respectively.

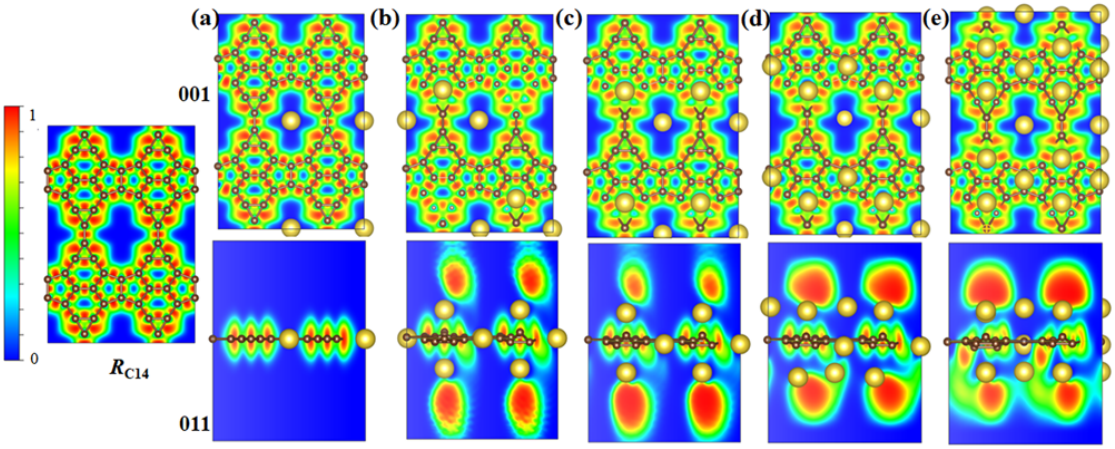

Figure S9. The ELF plots of the (001) and (011) slices for (a) Na_4C_{56} (b)Na_8C_{56} (c)$Na_{12}C_{56}$ (d)$Na_{20}C_{56}$ (e)$Na_{28}C_{56}$.

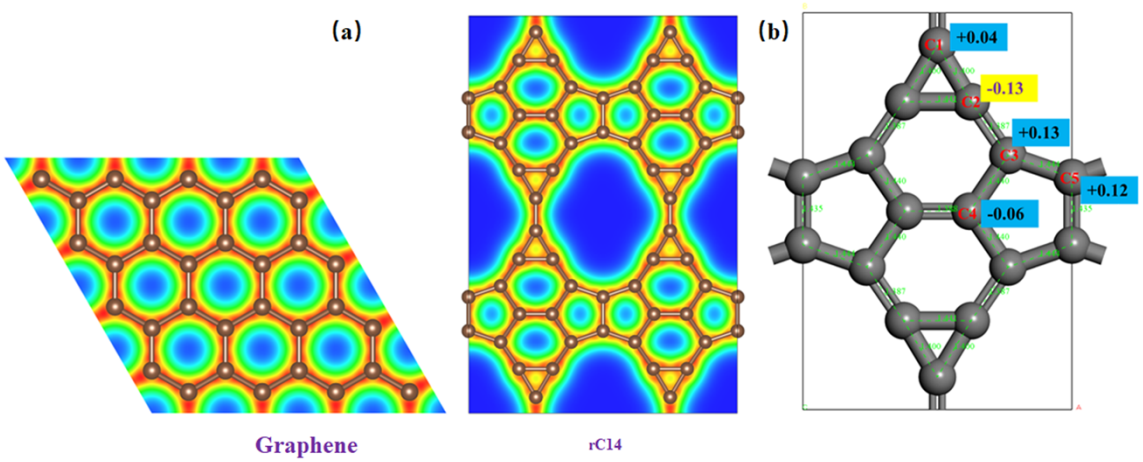

Figure S10. (a) The charge density of graphene and 2D rC14. The blue and red areas imply low and high electron localization, respectively. (b) Bader charge population analysis of rC14.

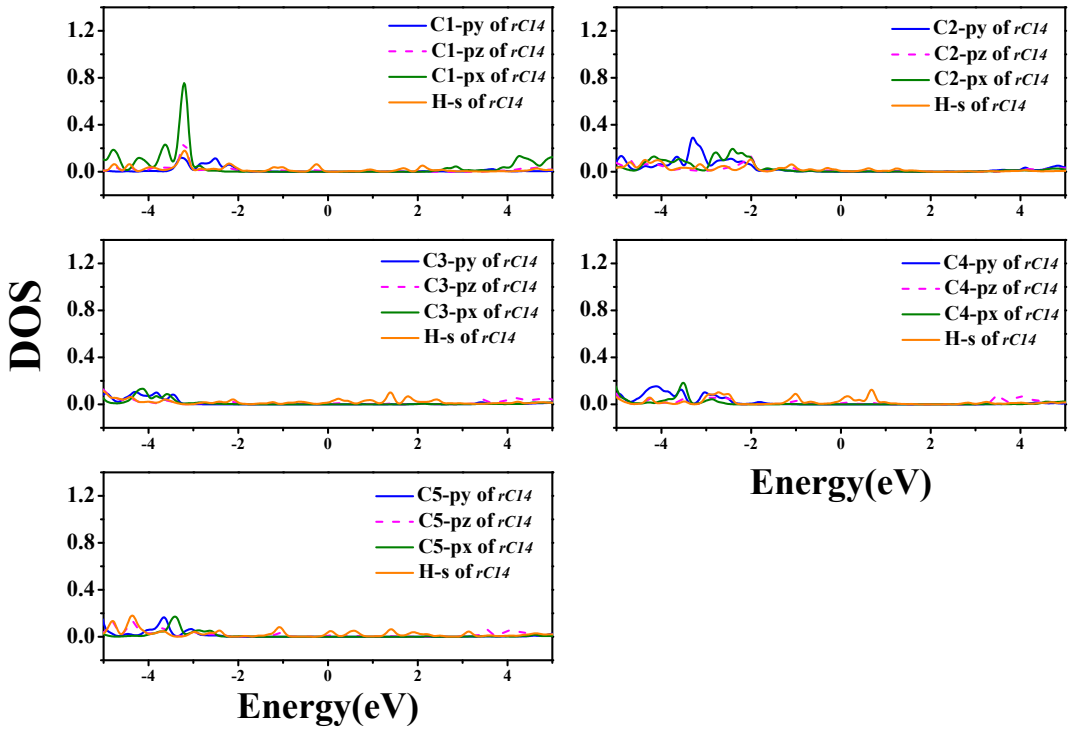

Figure S11. The Partial density of states (PDOS) of the C sites of 2D rC14.

Table S1. The optimized lattice parameters (a and b, c = 20 Å, and bond lengths $d_{C–C}$), and total energy E_{tot} of rC14. For comparison, the corresponding parameters for graphene, popgraphene, T-graphene, penta-graphene, phagraphene, Net-w, Biphenylene and graphdiyne are also provided.

Structure	Space group	a(Å)	b(Å)	$d_{C-C\ (Å)}$	E_t(eV/atom)	References
Graphene	$P6_3/mmc$	2.46	2.46	1.42	-9.23	[2]
	$P6_3/mmc$	2.46	2.46	1.42	-9.23	This work
Popgraphene	P2mg	3.68	9.11	1.40~1.46	-8.91	[4]
	P2mg	3.69	9.01	1.39~1.45	-8.90	This work
T-graphene	P4/mmm	4.87	4.87	-	-8.73	[5]
	P4/mmm	4.87	4.86	1.46,1.37	-8.71	This work
Penta-graphene	$P\text{-}42_1m$	3.64	3.64	1.34,1.55	-8.32	[6]
	$P\text{-}42_1m$	3.64	3.64	1.34,1.54	-8.33	This work
Phagraphene	Pmg	8.09	6.65	1.40~1.44,1.52	-9.03	[7]
	Pmg	8.11	6.64	1.39~1.43,1.52	-9.02	This work
Net-w	Cmmm	10.04	4.43	1.38~1.47	-8.85	[8]
	Cmmm	10.04	4.43	1.38~1.47	-8.85	This work
Biphenylene	Pmmm	4.52	3.77	1.41~1.46	-8.76	[9,10]
	Pmmm	4.52	3.77	1.41~1.46	-8.79	This work
graphdiyne	P6/mmm	9.46	9.46	1.22, 1.38, 1.43	-8.49	[11,12]
	P6/mmm	9.46	9.46	1.23, 1.39, 1.43	-8.48	This work
RC14-graphene	Pmmm	5.74	8.45	1.38~1.44	-8.59	This work

Table S2. The C–H bond distance, adsorption energy and bonding relationship between the active site and H atom.

Strain (%)	Bond length of C-H /Å	Adsorption energy /eV	ICOHP of C-H/eV
0	1.108/1.103/1.117/1.121/1.117	-0.093/-0.163/0.559/0.615/0.204	-6.001/-5.928/-5.758/-5.596/-5.749
-0.5	1.106/1.102/1.117/1.120/1.117	-0.206/-0.284/0.560/0.580/0.199	-6.028/-5.944/-5.782/-5.623/-5.753
-1	1.106/1.102/1.116/1.116/1.116	-0.410/-0.486/0.380/0.478/0.015	-6.056/-5.963/-5.805/-5.664/-5.766
-1.5	1.106/1.101/1.116/1.118/1.116	-0.702/-0.772/0.118/0.301/-0.242	-6.069/-5.980/-5.818/-5.699/-5.771
-2	1.105/1.100/1.115/1.117/1.115	-1.131/-1.178/-0.302/-0.010/-0.731	-6.087/ -5.992/-5.835/ -5.728/-5.791

References

1 G. Kresse and J. Furthmüller, *Phys. Rev. B: Condens. Matter Mater. phys.,* 1996, **54**, 11169-11186.

2 S. Hasan, T. Mehmet, E. Aktürk and S. Tuğrul, *Phys. Rev. B.*, 2009, **80**, 155453.

3 C. Z. Wang and K. M. Ho, *Phys. Rev. Lett.*, 1993, **71**, 1184-1187.

4 S. Wang, B. Yang, H. Chen and E. Ruckenstein, *J. Mater. Chem. A*, 2018, **6**, 6815–6821.

5 H. Huang, Y. Li, Z. Liu, J. Wu and W. Duan, *Phys. Rev. Lett*., 2013, **110**, 029603.

6 S. Zhang, J. Zhou, Q. Wang, X. Chen, Y. Kawazoe and J. Puru, *PNAS*., 2015, **112**, 2372-2377.

7 Z. Wang, X. Zhou, X. Zhang, Q. Zhu, H. Dong, M. Zhao and A. R. Oganov, *Nano Lett*., 2015, **15**, 6182–6186.

8 X. Wang, H. Li and J. Wang, *Phys. Chem. Chem. Phys*., 2013, **15**, 2024-2030.

9 Y. Luo, C Ren, Y Xu, J Yu, S Wang and M Sun, *Sci. Rep*., 2021, **11**, 19008.

10 M. A. Hudspeth, B. W. Whitman, V. Barone and J. E. Peralta, *ACS Nano*, 2010, **4**, 4565-4570.

11 J. Xu, Q. Wan, M. Anpo and S. Lin, *J. Phys. Chem.C*, 2020, **124**, 6624-6633.

12 J. Kim, S. Kang, J. Lim and W. Y. Kim, *ACS Appl. Mater. Interfaces*, 2019, **11**, 2677−2683